ELSEVIER

Colloids and Surfaces A: Physicochem. Eng. Aspects 214 (2003) 1–11

COLLOIDS AND SURFACES A

www.elsevier.com/locate/colsurfa

Flow of thin films on patterned surfaces☆

L. Kondic [a,*], J. Diez [b]

[a] *Department of Mathematical Sciences and Center for Applied Mathematics and Statistics, New Jersey Institute of Technology, Newark, NJ 07102, USA*

[b] *Instituto de Física Arroyo Seco, Universidad Nacional del Centro de la Provincia de Buenos Aires, Pinto 399, 7000 Tandil, Argentina*

Received 25 June 2001; accepted 15 August 2001

Abstract

We present fully nonlinear time-dependent simulations of the gravity driven flow of thin wetting liquid films. The computations of the flow down a homogeneous substrate show that the contact line where liquid, solid, and gas phase meet becomes unstable and develops patterns. These computations are extended to inhomogeneous surfaces, and show that inhomogeneity can induce instability of the fluid front. In particular, we analyze flow on patterned surfaces, where surface inhomogeneity is introduced in a controllable manner. We discuss the conditions that need to be satisfied so that surface patterns, lead to predictable selective wetting of the substrate. Applications of these results to technologically relevant flows are discussed.

Keywords: Thin fluid films; Instability; Patterned surfaces

1. Introduction

The flow of thin films is relevant in a number of different fields, such as engineering (microchip production), biology (lining of mammalian lungs), and chemistry (flow of surface active materials). These flows can be driven by gravitational (flow down an inclined plane), centrifugal (spin coating), or Marangoni forces. In many situations, the fluid fronts become unstable leading to formation of patterns (fingers or triangular saw-tooth patterns), and resulting in uneven or partial surface coverage. Very often, these instabilities are undesirable in technological applications since they may lead to formation of dry regions or other defects.

In this work, we concentrate on perhaps the simplest of these problems, the flow of a thin film down an inclined plane. This configuration still retains the most important aspects of the problem, while its relative simplicity allows for detailed theoretical, computational, and experimental analysis. One hopes that if this problem can be understood in detail, the analysis and the results can be extended to more involved configurations,

☆ This paper was omitted from the Special Issue from the Proceedings of the International Tri/Princeton Workshop on Nanocapillarity. Wetting of Hetereogeneous Surfaces and Porous Solids, which was held in Princeton, NJ, June 25–27, 2001 (Colloids Surf. A: Physiochem. Eng. Aspects volume 206).

* Corresponding author

E-mail address: kondic@m.njit.edu (L. Kondic).

0927-7757/02/$ - see front matter
PII: S0927-7757(02)00387-4

such as those involving flows on chemically etched substrates [1,2]. Another important reason for analyzing the gravity driven flow is that experiments are relatively easy to perform, so that the theoretical and computational results can be verified in a straightforward fashion. Further, the main results are scale-independent, allowing for rescaling of macroscopic experiments/simulations/theory to micro or even shorter scales (in the case where nanoscales become relevant, one needs to include contact line tension (see, e.g. Pompe [3])).

Experiments are usually performed by releasing fluid in some controllable fashion at the top of an incline. After some time, the initially straight contact line, where liquid, gas, and solid phase meet, becomes unstable with respect to transverse perturbations. It has been conjectured that this instability is related to the formation of a capillary ridge in the fluid profile, just behind the advancing contact line. Silvi and Dussan [4] expanding on the pioneer work by Huppert, [5] showed that the wetting properties of the fluid played an important role in instability development and the degree of the surface coverage. Very recently, the experiments by Johnson [6] and Johnson et al. [7], as well as the computations by Diez and Kondic [8,9] show that another important parameter is the inclination angle; since it influences not only the rate of growth of the patterns, but also modifies their shape.

Theoretical analysis of the problem requires, in the first place, resolving the so-called 'contact line paradox'. As it is well known, assuming standard no-slip boundary condition at the contact line leads to a divergence of energy dissipation (see e.g. Dussan [10] de Gennes [11] or Haley and Miksis [12]). This problem is typically approached by either relaxing the no-slip boundary condition, or by assuming the presence of a thin precursor film in front of the propagating contact line. Both approaches introduce a short length scale into the problem, thus requiring analysis of the influence of this additional parameter on the stability.

The dynamics of the main body of the fluid film is typically approached using lubrication approximation. Within this framework, an initial insight into the instability results from the linear stability analysis (LSA). Troian et al. [13] perform LSA for the flow down a vertical plane and show that there is a band of unstable modes, with short wavelengths stabilized by surface tension. Bertozzi and Brenner [14] extend the analysis to the general case of the flow down an inclined plane, and show that the normal component of gravity (hydrostatic term) shifts the mode of maximum growth to longer wavelengths, and also tends to stabilize the flow by decreasing the growth rate of the instability. This stabilizing effect appears to be so strong that it completely removes the instability for very small inclination angles, in contradiction to experiments. The work by Bertozzi and Brenner [14], as well as a very recent work by Ye and Chang [15], attribute this discrepancy to the fact that the surface itself is not perfect, and analyze how noise could propagate from the substrate to the fluid front and lead to instability.

Our previous works [8,9] analyze instability development in the flow of thin films on homogeneous surfaces. In this work, we concentrate on the influence of heterogeneity of the surface on the instability development, with particular emphasis on the flow on patterned surface and resulting selective wetting. This study is partially motivated by an earlier work by Kondic and Bertozzi [16] which has shown that perturbations of the substrate can play a significant role in development of instability. However, in [16] this conclusion is reached indirectly, by observing the influence that a perturbation of the substrate has on the height of the capillary ridge, which is itself related to the instability development. Here, we report results of fully nonlinear simulations in $2+1$ space dimensions (thickness of the fluid is averaged over within the framework of lubrication approximation). Although our simulations concentrate on the gravity driven flow of macroscopic thin films, the results are closely related to the recent microscale experiments of thermally driven flow on patterned silicone wafers substrates [1,2].

2. Formulation of the problem

Dynamics of thin liquid films is typically analyzed within the framework of lubrication approximation. The assumptions of this approach,

as well as the details of our computational methods are given elsewhere [8,9,17]. For completeness, here we give the basic outline, and refer the interested reader to these earlier works for details.

Within the lubrication approximation, the velocity of the fluid is depth-averaged over the thickness of the film (see e.g. Greenspan [18]). Following this approach, one obtains the average fluid velocity, $\mathbf{v}=(u, v)$,

$$\mathbf{v}=-\frac{h^2}{3\mu}[\nabla p-\rho g \sin\alpha\mathbf{i}], \tag{1}$$

where $\nabla=(\partial_x, \partial_y)$, h is the fluid thickness, p the pressure, μ the viscosity, ρ the density, g the gravity, and α is the inclination angle of the plane of the substrate. The coordinate frame is chosen so that $\mathbf{i}$ points down the incline, and $\mathbf{j}$ is the transverse direction in the plane. We note that Eq. (1) assumes no-slip boundary condition at the fluid−solid interface. The pressure includes the hydrostatic component, and the contribution following from the Laplace–Young boundary condition at the fluid–air interface

$$p=-\gamma\nabla^2 h+\rho g h\cos\alpha, \tag{2}$$

where γ is the surface tension. Assuming fluid incompressibility, the continuity equation gives

$$\frac{\partial h}{\partial t}=-\nabla(hv)$$

$$=-\frac{1}{3\mu}\nabla[\gamma h^3\nabla\nabla^2 h-\rho g h^3\nabla h\cos\alpha$$

$$+\rho g h^3\sin\alpha\mathbf{i}]. \tag{3}$$

To balance viscous and capillary forces in Eq. (3), we scale h by the fluid thickness far behind the contact line, h_c, and define the scaled in-plane coordinates and the time by $(\bar{x}, \bar{y}, \bar{z})=(x/x_c, y/x_c, t/t_c)$, where

$$x_c=\left(\frac{a^2 h_c}{\sin\alpha}\right)^{1/3}, \qquad t_c=\frac{3\mu}{\gamma}\frac{a^2 x_c}{h_c^2\sin\alpha}, \tag{4}$$

and $a=\sqrt{\gamma/\rho g}$ is the capillary length. The velocity scale is chosen naturally as $U=x_c/t_c$, and the capillary number is defined as $Ca=\mu U/\gamma$. Using this nondimensionalization, Eq. (3) for $\bar{h}=h/h_c$ is given by (dropping the bars)

$$\frac{\partial h}{\partial t}+\nabla[h^3\nabla\nabla^2 h]-D(\alpha)\nabla[h^3\nabla h]+\frac{\partial h^3}{\partial x}=0, \tag{5}$$

where the single dimensionless parameter $D(\alpha)=(3Ca)^{1/3}\cot(\alpha)$ measures the size of the normal component of gravity. In this work we mainly concentrate on the flow down a vertical plane, where $D=0$.

As mentioned in the Section 1, all the theoretical and computational methods require some regularizing mechanism—either assumption of a small foot of fluid in front of the apparent contact line (precursor film, see the works by Troian et al. [13], Bertozzi and Brenner [14] or Spa and Homsy [19]), or relaxing the no-slip boundary condition at fluid–solid interface (see e.g. Greenspan [18] Dussan [20] or Hocking and Rivers [21]). Diez et al. [17] have recently performed an extensive analysis of the computational performance of these regularizing mechanisms applied to the spreading drop problem. In that paper it is shown that the results are rather insensitive to the choice of the model, consistently with, e.g. Spa and Homsy [19]. However, the computational performance of the precursor film model is shown to be much better than that of various slip models. For this reason, in this work we also use a precursor film of thickness b_0 (scaled by h_c) as a regularizing method.

The computational domain is chosen as a rectangle defined by $0\le x\le L_x$ and $0\le y\le L_y$ which is divided into $N_x\times N_y$ node points (x_i, y_j) with $i=1, \ldots, N_x$ and $j=1, \ldots, N_y$. Eq. (5) is then discretized in space using a central finite difference scheme. The boundary conditions are chosen to model constant fluid flux far behind the fluid front. That is, we assume that there is an infinite stream of fluid far behind the front that keeps the fluid height constant there. Within our nondimensionalization scheme, this leads to $h(0, y, t)=1$. We require that far ahead of the moving front, the fluid height is equal to the precursor thickness, $h(L_x, y, t)=b_0$, and also that the streamwise gradients of the fluid height vanishes there, i.e. $h_x(0, y, t)=h_x(L_x, y, t)=0$. At the side boundaries $y=0$ and $y=L_y$, it is convenient to use $h_y(x,$

$0, t) = h_y(x, L_y, t) = 0$, $h_{yyy}(x, 0, t) = h_{yyy}(x, L_y, t) = 0$. This choice enforces no-flow across these boundaries. Since the tangential component of the fluid flux is let free, these boundaries could be thought of as 'slipping walls'. Due to the fact that odd derivatives are set to zero there, the boundaries can be also considered as symmetry planes.

Time discretization is performed using implicit Crank–Nicolson scheme. The advantages of an implicit scheme for this problem are obvious: the stability requirement for an explicit scheme is that $\Delta t < C\min[\Delta x, \Delta y]^4$, where Δt is a time step, and C is a positive constant. Thus, an explicit scheme requires very short time steps for a reasonable spatial accuracy. The nonlinear system of algebraic equations that results after time discretization is linearized using Newton method; the linearized problems are then solved using iterative biconjugate gradient method. Clearly, the simulations are computationally intensive, so that significant effort has been put in producing an efficient method. More details regarding efficiency, computational cost, and other issues such as convergence and accuracy of our method are given in [8,9].

3. Stability of the flow

LSA [13,14,19] of the governing Eq. (5) has showed that the flow is unstable with respect to perturbations of the fluid front in the transverse direction. LSA is performed by expanding to the first order all the nonlinear terms in Eq. (5) about the base state, which is obtained by assuming that the fluid profile is y-independent. Fig. 1 shows the base states for two values of the precursor film thickness, resulting from the simulations of Eq. (5), where it is assumed that $h = h(x, t)$ only. We note the presence of the capillary ridge just behind the advancing contact line and recall that it is closely related to the instability development [13,14,19]. By comparing Fig. 1(a and b), we observe that the capillary ridge is increased in size as the precursor thickness b_0 is decreased. Recent experiments by Ye and Chang [15] show that the instability could be significantly enhanced if b_0 is decreased; correspondingly, one can conjecture that there is strong correlation between the height of the capillary ridge and the instability of the flow; we will use this observation in what follows. For later reference we note that the fluid flows slower as b_0 is decreased, since smaller b_0 provides more resistance to the flow. This is intuitively obvious since the limit $b_0 \to 0$ is singular; in the limiting case $b_0 = 0$, no-slip boundary condition would not allow for any dynamics in the contact line region.

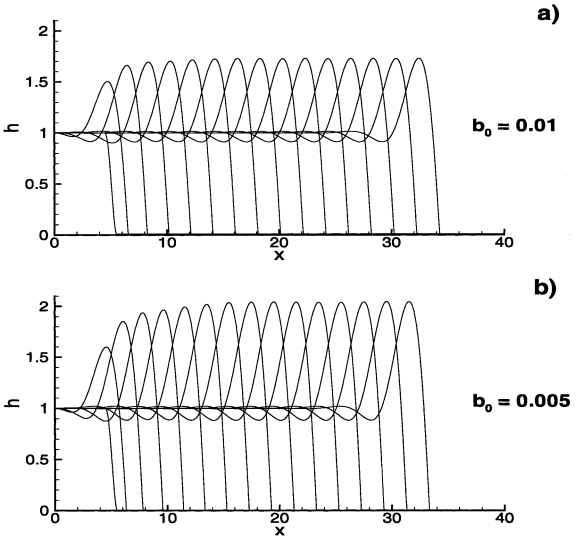

Fig. 1. Snapshot of the fluid profiles in $\delta t = 2$ intervals ($D = 0$). The only difference between (a) and (b) is the precursor film thickness which is $b_0 = 0.01$ (a) and $b_0 = 0.005$ (b).

Going back to LSA, we note that the surface tension (responsible for the fourth order term in Eq. (5)) suppresses the instability of short wavelengths, while the component of the gravity in the downhill direction plays destabilizing role. As a results, there is a critical wavelength, λ_c, where stability changes from unstable to stable (we note that $\lambda = \infty$ is marginally stable as a consequence of translational invariance of the unperturbed system). Although LSA is valid for short times only, one expects that the distance between resulting patterns in actual experiments is close to the wavelength of maximum growth, λ^*, from LSA. For future reference, we note that $\lambda_c \approx 8$ and $\lambda^* \approx 14$ for $D = 0$ [13].

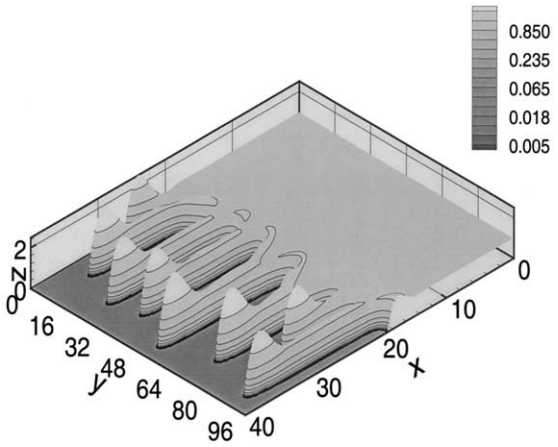

Fig. 2. Contour plot of the fluid thickness. Initial profile is perturbed by a superposition of 50 modes characterized by random amplitudes. Here $D=0$ and $b=0.01$. Note that the z scale is considerably stretched for presentation purposes.

Our computational results [8,9] for the flow down a homogeneous surface confirm the main predictions of LSA. Fig. 2 shows an example of these results, where the fluid front has been perturbed at $t=0$ by a superposition of $N=50$ modes characterized by random amplitudes and wavelengths $\lambda_{0,i}=2L_y/i$, $i=1, \ldots, 50$. The main result relevant to the discussion that follows is that the resulting distance between the developed patterns is nonuniform, although it is on average relatively close to λ^* from LSA (additional simulations which use different distributions of initial wavelengths and different domain size show that this average value is close to 12). This nonuniformity is not a consequence of, for example, the boundary conditions (in the simulations, the boundaries are perfect), but it is an intrinsic property of the flow.

LSA (and the computations mentioned above [8,9]) assume presence of small perturbations of the contact line in the transverse direction, that are necessarily present in any physical experiment. Let us, however, ignoring these perturbations, assume that the position of the fluid front is initially y-independent, and discuss the influence that perturbations of the surface itself can have on the stability of the flow. In this work, we model these perturbations by perturbing the thickness of the precursor film. While it might appear that imposing perturbations of this kind is rather restrictive since a precursor film is not always present in physical experiments or technological applications, this approach is actually quite general. As mentioned earlier, a number of works [11,17,19] have shown that the main features of the flow are not influenced significantly by the choice of the regularizing method at the contact line; for the macroscopic flow properties (in particular, instability development), the main factor is the actual length-scale that is introduced at the front, and not the regularizing method itself. This length-scale determines the degree of energy dissipation at the front, and one expects that its spatial variation can have significant influence on the macroscopic flow properties. We note that spatially dependent slip coefficient was used some time ago by Hocking [22] and more recently in weakly nonlinear analysis by Hoffman et al. [23].

In a recent work, Kondic and Bertozzi [16] analyzed the influence that a localized perturbation of the precursor thickness has on the flow in 1D geometry (the y direction is ignored). Fig. 3 shows an example of these results: as the main body of the fluid flows over a perturbation (imposed at $x=20$ in Fig. 3), the height of the capillary ridge is increased, implying, as pointed out above, that the stability properties of the flow may be modified. Correspondingly, it is reasonable to assume that surface inhomogeneities (which we model by perturbing precursor thickness) might lead to flow instabilities. Fig. 3 shows that a small perturbation of the precursor film (see inset) is significantly amplified; modification of the precursor on the scale of 1% of the thickness of the main body of the fluid leads to large changes of the height of the capillary ridge. We note that only perturbations that are sufficiently wide influence significantly the height of the capillary ridge [16]. This result is similar to the solutions of rather different problem: planarization during spin coating over perturbations (trenches) whose depth is of the same order as the thickness of the main body of the fluid [24] (the perturbations considered here are much more shallow).

Now we concentrate on using this extreme sensitivity of the macroscopic flow to small perturbations of the precursor to produce ‘con-

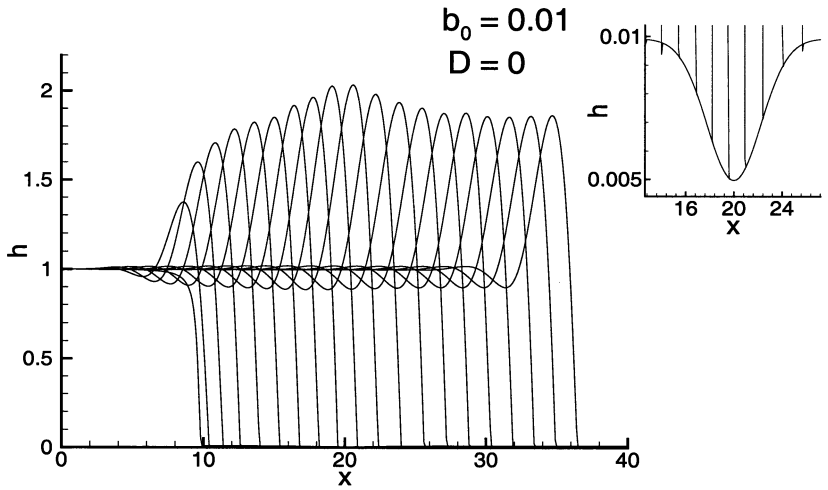

Fig. 3. Snapshot of the 1D fluid profile as it flows over a precursor perturbation. Th inset shows the perturbation itself (note different scale).

trollable' instability. The main idea is that one could prepare the surface in such a way that the instability that develops resembles the effects of a selective wetting mechanism, as in the recent microscopic experiments [1,2]. In these experiments, the patterned surface (alternating stripes of bare and coated SiO_2), is prepared in a rather elaborate fashion, and the flow is driven by thermocapillary shear stress at the air–liquid interface. Correspondingly, the problem is much more complicated (and characterized by much shorter length-scales) than the gravity driven flow outlined here. However, due to the similar nature of instability in these two problems, one expects that it shall be possible to prepare a macroscopic experiment in which the stripes (or any other desired patterns) are imposed on the base surface in some simple manner that allows for relatively straightforward experiments.

From modeling point of view, one also desires to introduce perturbations in some simple manner. In the microscopic experiments mentioned above [1,2], the perturbations result from different (hydrophilic/hydrophobic) wetting properties of the stripes made out of different materials. Modeling a flow where fluid wetting properties are nonuniform would require significantly more involved computational and theoretical methods, since an additional variable, the contact angle, comes into play. However, we may use the fact that an important aspect of the flow on a surface characterized by different wetting properties is that the fluid prefers flowing on the hydrophilic portions. In the simulations, we can achieve similar effect by modifying the precursor film thickness, since this parameter defines resistance to the flow, as it can be seen in Fig. 1. Correspondingly, we model the patterned substrate by modifying the precursor film thickness appropriately. While the manner in which the perturbations are imposed definitely influences the details of the flow, one hopes that relatively crude modeling of surface heterogeneity by modifying the precursor film still provides good insight into the main aspects of the flow. This is subject of the next section.

4. Flow on patterned surfaces

In what follows, we modify the precursor by imposing 'channels' in the streamwise direction. Fig. 4 shows these channels: they have flat central region of a given depth, δ (in the units of b_0), and a transition region surrounding the flat part and providing smooth change from the channels' bottoms to the unperturbed precursor. These transition regions are needed since lubrication approximation assumes weak gradients of the fluid

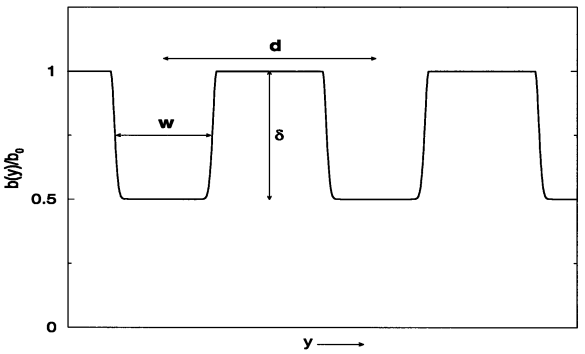

Fig. 4. Cross section of the channels imposed on the precursor film.

thickness, with which a sharp interface between channels and unperturbed precursor would not be consistent. On the sides of the channels, the precursor thickness of these regions is specified as $b(y) = b_0[1 - \delta \exp(-w_t(y - y_c)^2)]$, where w_t defines the width of the transition region, and y_c is the position of the edge of the bottom part of a channel. We note that the results are almost insensitive to the particular functional form, or to the value given to w_t; we typically use $w_t = 4$, which gives reasonable (order 1) width of the transition region. There is also analogous transition area in front of the channel. In the results that follow, we define the effective width of the channels, w, as the width of the region in which the precursor thickness is less than $b_0(1 + \delta)/2$ (see Fig. 4).

Fig. 5 shows an example of our results for the flow down a vertical plane ($D = 0$), and unperturbed $b_0 = 0.01$. At $t = 0$, the time evolution is started using the initial condition obtained from 1D simulations shown in Fig. 1(a). The precursor film is thinner in the channel region, so, as mentioned earlier, there is more resistance to the flow there. The fluid preferentially flows in the 'easy' flow region in between the channels. As a result, finger-like patterns form, similarly to the results shown in Fig. 2, where the contact line itself is perturbed. There are, however, significant differences between the results shown in Figs. 2 and 5. First, the flow over perturbed precursor is characterized by uniform distance between the fingers, which also all grow at the same rate (as

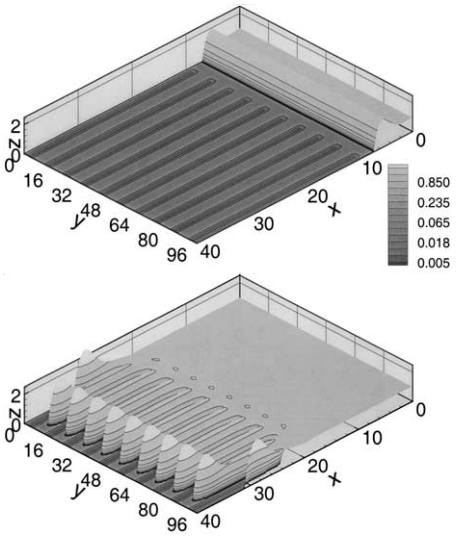

Fig. 5. Contour plot of the fluid as it flows over striped substrate. The part (a) shows the initial configuration, and the part (b) shows well developed fingers that propagate between the channels. Effective width of the channels is $w = 3.5$, and the distance between their centers is $d = 10$. Other parameters are as in Fig. 2. Note that $y = 48$ is the symmetry line.

they should, since there is no element of randomness in these simulations). Second, the distance between the fingers in Fig. 5 is determined by the imposed 'wavelength', or distance, d, between the precursor perturbations ($d = 10$ in Fig. 5). On the other hand, the average distance between the fingers shown in Fig. 2 is about 12. We note that in Fig. 5 and the later figures, the channels are arranged in such a way that $y = 48$ is the symmetry line; consequently, all the results are symmetric with respect to the middle of the domain. The distance from the outermost channels to the domain boundaries ($y = 0,96$) can vary, and this variation is responsible for different growth of the boundary fingers in Fig. 5 and the following figures.

Similar results to those shown in Fig. 5 have been observed in the experiments on chemically etched silicon wafers [1,2]. In these experiments, it is also observed that there are limits to how closely to each other the fingers can be made to flow. In what follows, we verify that our simulations can reproduce this effect, and also analyze the importance of various parameters that influence the

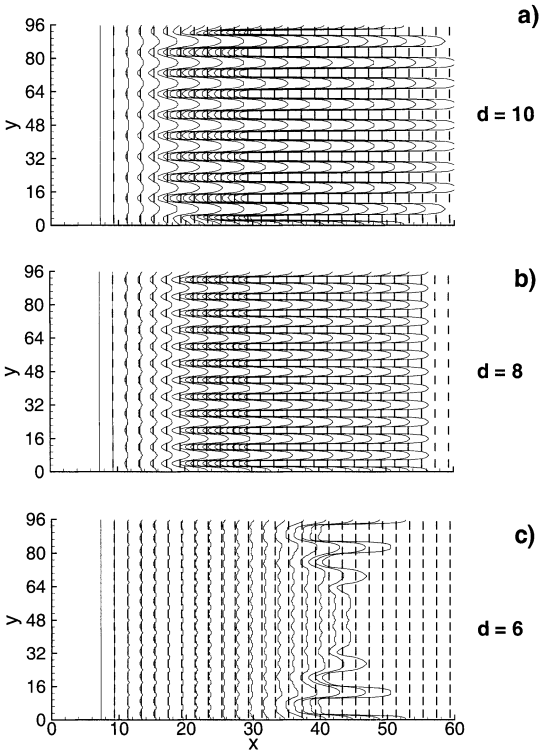

Fig. 6. Snapshots of the fluid profiles in $\delta t = 2$ intervals. Effective width of the channels (the regions covered by small circles) is $w = 3.5$, and the distance between the centers of the channels is $d = 10$, 8, 6 in (a), (b) and (c), respectively. Other parameters are as in Fig. 5, the results are symmetric with respect to $y = 48$, as explained in the text.

flow. In particular, we explore whether it is only the imposed d that is important in determining the flow, or whether it is also the relative width of the channel region compared with the unperturbed precursor region that matters.

Fig. 6 shows the snapshots of the fluid fronts as d is decreased from $d = 10$ (a) to $d = 8$ (b) and $d = 6$ (c). By comparing the results shown in (a) and (b) we notice that the fingers in the case (a) propagate faster compared with (b); this result can be explained qualitatively based on LSA that predicts larger growth rates for $\lambda = 10$ compared with $\lambda = 8$. In the case (c), the fluid does not follow the pattern imposed by the surface. To understand this result, let us recall that LSA predicts change in stability about $\lambda_c = 8$, which is also the wavelength imposed by the precursor at which we observe transition in the flow behavior. We conclude that for $d \lesssim 8$, the surface tension prevents the fluid from following the imposed patterns. However, even for $d \lesssim 8$, the imposed surface patterns do lead to instability, but characterized by rather irregular growth rates and separation of the patterns. The fingers still tend to follow easy flow regions, but this tendency is in obvious competition with capillary forces; average emerging distance between the fingers is about 12, which is the same as in the case of the flow on unperturbed precursor where random noise is superimposed on the initial profile[1], shown in Fig. 2.

Next, we analyze how relative widths of the channel and the unperturbed region influence the flow. Fig. 7 shows the results where $d = 8$, and the effective channel width is changed from $w = 2.5$ (a) to $w = 5.5$ (b) ($w = 3.5$ in Fig. 6). While there is no significant difference in the results, we observe, perhaps surprisingly, that there is a particular channel width for which finger tips propagate the fastest (this is $w = 3.5$ among the cases presented here). This result can be qualitatively explained as

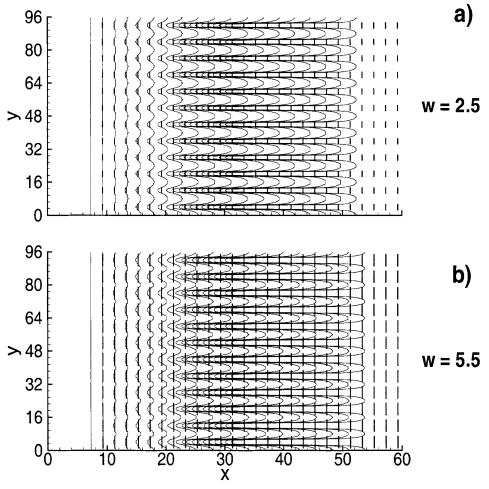

Fig. 7. Snapshots of the fluid profiles in $\delta t = 2$ intervals. The distance between the channels is $d = 8$, and the effective widths are $w = 2.5$ and 5.5 in (a) and (b), respectively ($w = 3.5$ is shown in Fig. 6(b)). Other parameters are as in Fig. 5.

[1] We note that channel pattern used in Fig. 6c is slightly different at $y = 3D(0,96)$. See [25] for more details.

follows. If the width of easy flow regions, $d-w$, is small, fluid as a whole is slowed down significantly by the channels. If, on the other hand, the width of the channels, w, is small, the channels do not slow down the fluid enough to produce large growth rate of the fingers. Of course, in the limits $w \to 0$, or $w \to d$ the fingers disappear completely.

Another consequence of having rather narrow regions of easy flow (small $d-w$) is that the width of the fingers is being slightly reduced if $d-w$ is less than the natural finger width, which can be estimated, e.g. from Fig. 2. We note that we have not observed any influence of the relative width of easy and difficult flow regions (i.e. $(d-w)/d$) on the distance between the emerging fingers. We have also performed simulations with different channel depths, with the main result that deeper channels enhance the finger formation and growth, as expected.

Next question to ask is what happens if the distance between the channels is considerably larger than the wavelength of critical growth, λ_c. In our simulations of flow on uniform surfaces, we have observed that if the contact line is perturbed with very long wavelengths, superharmonic frequencies can be excited through nonlinear mode (self) interaction [9]. Naturally, one could expect similar effect in the flow on a patterned surface. Indeed, Fig. 8 shows that this is exactly what happens. In Fig. 8(a), where $d = 20$ we observe the beginning of excitations of modes characterized by shorter wavelengths; however, continuous channel presence suppresses this instability. The result is that there is still a single finger in each easy flow region between the channels. On the sides of the computational domain, where there is more space available for growth, shorter wavelengths (i.e. more than one finger) develop. In Fig. 8(b), however, $d = 30$ leaves enough space for the development of three fingers in each of easy flow regions. Interestingly enough, the figure shows that initially two fingers develop, and than 'secondary' instability leads to appearance of the third one.

Until now, we have concentrated on the fluid flow down a vertical plane. If the surface is inclined, it is known that the instability is reduced, the shape of the patterns is changed from finger-like to triangular ones, and the critical wavelength is shifted to longer wavelengths (see [8,9] and the references therein). Therefore, if our assumption that the capillary forces are responsible for the change in the flow pattern as the channels are shifted closer to each other (viz. Fig. 6) is correct, then this effect should be modified as D is increased.

Fig. 9 shows the fluid fronts for $D = 1$, and $d = 10$ (a), and $d = 8$ (b). Here we show the flow for longer times ($\delta t = 10$ between the consecutive

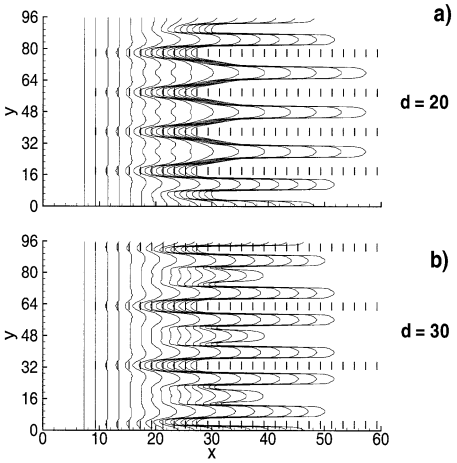

Fig. 8. Snapshots of the fluid profiles in $\delta t = 2$ intervals for large distance between the channels: $d = 20$, 30 in (a) and (b), respectively. All other parameters are as in Fig. 5.

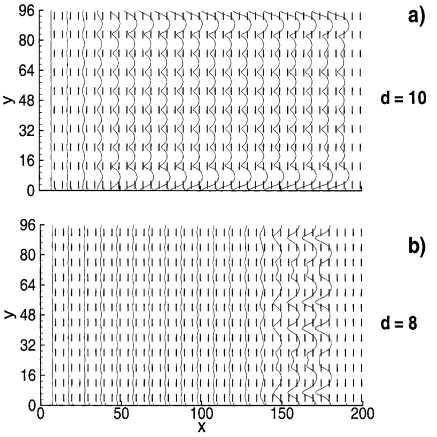

Fig. 9. Snapshots of the fluid profiles in $\delta t = 2$ intervals for the flow down an inclined plane ($D = 1$). Here $d = 10$ (a) and $d = 8$ (b). All other parameters are as in Fig. 5.

snapshots), and in longer domain (200, compared with 60 for $D=0$). Obviously, the instability is much weaker compared with $D=0$ case. What is more interesting is that for $d=10$ (Fig. 9(a)), we note deviation from perfect periodicity that is different from the $D=0$ case (viz. Fig. 6(a)). For $d=8$, periodicity of the imposed substrate has been lost, and the front parts of the triangular fluid patterns follow only every second of the easy flow regions (Fig. 9(b)). Since for this d the flow down a vertical plane does follow the periodicity of the substrate (viz. Fig. 6(b)), this result clearly shows that there is consistency between a shift of λ_c in LSA and the minimum distance between the channels as D is increased. Due to the fact that surface tension is important factor that determines λ_c, we conclude that one may use a fluid characterized by lower surface tension, if the goal is to produce closely spaced patterns. The manner in which other fluid and flow variables influence this minimum distance can be readily obtained from the scales used to nondimensionalize the governing Eq. (5), see Eq. (4). Presumably the same ideas can be extended to other similar flows (see [1] for an example).

5. Conclusion

In this paper, we present computational results that outline the connection between natural instability of gravity driven thin liquid films on homogeneous surfaces, and the flow of thin films on patterned (stripped) surfaces. Heterogeneity of the surface is modeled by varying the thickness of the precursor film. An important observation is that, even in this relatively simple model, one can obtain very similar results as in the related, but much more involved recent experiments of the flow on etched silicon wafers, driven by thermocapillary shear stresses [1]. In our system, we find that the shortest attainable distance between consecutive fingers is approximately equal to the critical wavelength obtained from LSA. Further, we find that this shortest distance is not significantly influenced by the relative widths of easy and difficult flow regions, although the finger widths, and the growth rates of propagating fingers might be influenced.

Another interesting result involves the flow on patterned surfaces where the wavelength imposed by the surface is larger than the wavelength of maximum growth from linear stability theory. In that case, we find that the presence of channels prevents the formation of multiple fingers in the easy flow region, although for very large distance between the channels, these multiple fingers do form.

While the gravity driven flow of thin liquid films is rather simple, it is closely related to technologically more relevant flows, such as spin coating, dip coating, Marangoni driven flows, etc. We expect that thorough understanding of this simple flow will also improve our understanding of these other more involved flow geometries, as well as of their applications.

Acknowledgements

J. Diez acknowledges Fullbright Foundation, NJIT, and Consejo Nacional de Investigaciones Científicas y Técnicas (CONICET-Argentina) for supporting his visit to NJIT, and L. Kondic support from NSF grant No. INT-0122911 and NJIT grant No. 421210.

References

[1] S.M. Troian, Nature 203 (1998) 335.
[2] A.A. Darhuber, S.M. Troian, J.M. Davis, S.M. Miller, S. Wagner, J. Appl. Phys. 88 (2000) 5119.
[3] T. Pompe, S. Hermighaus, Phys. Rev. Lett. 85 (2000) 1930.
[4] N. Silvi, E.B. Dussan, V, Phys. Fluids 28 (1985) 5.
[5] H. Huppert, Nature 300 (1982) 427.
[6] M.F.G. Johnson, Experimental study of rivulet formation on an inclined plate by fluorescent imaging, Ph.D. thesis, Northwestern University, 1997.
[7] M.F.G. Johnson, R.A. Schluter, M.J. Miksis, S.G. Bankoff, J. Fluid Mech. 394 (1999) 339.
[8] J. Diez, L. Kondic, Phys. Rev. Lett. 86 (2001) 632.
[9] L. Kondic, J. Diez, Phys. Fluids 13 (2001) 3168.
[10] E.B. Dussan, V, Annu. Rev. Fluid Mech. 11 (1979) 317.
[11] P.G. de Gennes, Wetting: statics and dynamics, Rev. Mod. Phys. 57 (1985) 827.

[12] P.J. Haley, M.J. Miksis, J. Fluid Mech. 223 (1991) 57.
[13] S.M. Troian, E. Herbolzheimer, S.A. Safran, J.F. Joanny, Europhys. Lett. 10 (1989) 25.
[14] A.L. Bertozzi, M.P. Brenner, Phys. Fluids 9 (1997) 530.
[15] Y. Ye, H. Chang, Phys. Fluids 11 (1999) 2494.
[16] L. Kondic, A.L. Bertozzi, Phys. Fluids 11 (1999) 3560.
[17] J. Diez, L. Kondic, A.L. Bertozzi, Phys. Rev. E 63 (2001) 0112081.
[18] H.P. Greenspan, J. Fluid Mech. 84 (1978) 125.
[19] M.A. Spaid, G.M. Homsy, Phys. Fluids 8 (1996) 460.
[20] E.B. Dussan, V, J. Fluid Mech. 77 (1976) 665.
[21] L.M. Hocking, A.D. Rivers, J. Fluid Mech. 121 (1982) 425.
[22] L.M. Hocking, J. Fluid Mech. 76 (1976) 801.
[23] K. Hoffmann, B. Wagner, A. Münch, in: H.J. Bungartz, F. Dust, C. Zenger (Eds.), Lecture Notes in Computational Science and Engineering, vol. 3, Springer, Berlin, 1999.
[24] L.E. Stillwagon, R.G. Larson, Phys. Fluids A 2 (1990) 1937.
[25] L. Kondic., J. Diez, Phys. Rev. E. 65 (2002) 045301.